QUARTERLY JOURNAL OF THE ROYAL METEOROLOGICAL SOCIETY
Q. J. R. Meteorol. Soc. **135**: 922–934 (2009)
Published online 28 April 2009 in Wiley InterScience
(www.interscience.wiley.com) DOI: 10.1002/qj.420

Measurements of aerosol properties from aircraft, satellite and ground-based remote sensing: A case-study from the Dust and Biomass-burning Experiment (DABEX)

B. T. Johnson,[a]*,† S. Christopher,[b] J. M. Haywood,[a],† S. R. Osborne,[a],† S. McFarlane[c] C. Hsu,[d] C. Salustro[d,e] and R. Kahn[d]

[a]*Met Office, Exeter, UK*
[b]*University of Alabama, Huntsville, AL, USA*
[c]*Pacific Northwest National Laboratory, Richland, Washington, USA*
[d]*Goddard Space Flight Center, Greenbelt, Maryland, USA*
[e]*Science Systems and Applications, Inc., Lanham, Maryland, USA*

ABSTRACT: This paper presents aircraft measurements of aerosol optical properties and radiative effects from the Dust and Biomass-burning Experiment (DABEX) over West Africa. On 19 January 2006 cloud-free skies and high aerosol loading provided ideal conditions for an intercomparison of aircraft, satellite and ground-based remote sensing instruments. Aerosol size distributions, optical properties, aerosol optical depth (AOD) and downwelling solar radiation were measured by the UK FAAM aircraft in the region of Niamey, Niger. The aircraft *in situ* measurements showed a mixture of dust and biomass-burning aerosols and indicated an AOD of 0.79 (at 550 nm) that compared well against AODs from the Banizoumbou Aerosol Robotic Network (AERONET) site (0.74) and a Microtops sunphotometer (0.72). AERONET size distributions showed a good degree of similarity with the aircraft *in situ* measurements. AERONET single-scattering albedos were also in fairly close agreement with the aircraft, having values of 0.85 and 0.87, respectively (at 550 nm). Measurements of downwelling solar radiation from the aircraft compared well with measurements from the Atmospheric Radiation Measurement (ARM) Mobile Facility (AMF) at Niamey. Radiative transfer modelling suggested a 130–160 W m^{-2} instantaneous reduction of downwelling solar radiation by the aerosol column (15–18% of the total flux). Measurements of downwelling solar radiation compared reasonably well against radiative transfer modelling based on the aircraft *in situ* data. Satellite retrievals of AOD from MISR and MODIS Deep Blue were within 0.05 of the ground-based sunphotometers measurements although there were discrepancies in optical properties retrieved by MISR, as compared to AERONET and the aircraft.

KEY WORDS aircraft measurement; AERONET; MODIS; MISR; optical properties

Received 30 October 2008; Revised 25 February 2009; Accepted 11 March 2009

1. Introduction

Aerosols scatter and absorb solar radiation and have a direct effect on the Earth's radiative energy budget. The scattering of solar radiation back to space leads to a cooling of the climate system whereas absorption by aerosols leads to a local heating of the atmosphere. Globally, aerosols are understood to exert a cooling influence since scattering is the more dominant process (IPCC, 2007). However, model estimates of the direct radiative forcing by aerosols vary depending on many factors, including the global distribution of aerosol optical depth (AOD), the representation of aerosol optical properties, and the vertical distribution of aerosols in the atmosphere. The development of satellite remote sensing and ground-based sunphotometer networks such as Aerosol Robotic Network (AERONET) over the past ten years has greatly increased opportunities for the validation of global aerosol transport models and observation-based constraints on the total direct radiative forcing by aerosol. With a growing reliance on remote-sensing methods for quantifying the impact of aerosols on climate, it is important to assess the performance of such retrieval algorithms against independent field measurements, including *in situ* measurements from aircraft.

Intensive measurements of dust and biomass-burning aerosol were made by the UK Facility for Airborne Atmospheric Measurements (FAAM) aircraft during the Dust and Biomass-burning Experiment (DABEX). This experiment took place from 13 January to 3 February 2006, in the region surrounding Niamey, Niger (West Africa). DABEX was part of the African Monsoon Multi-disciplinary Analysis (AMMA) dry season special

*Correspondence to: B. T. Johnson, Met Office, FitzRoy Road, Exeter, EX1 3PB, UK. E-mail: ben.johnson@metoffice.gov.uk
†The contributions of B. T. Johnson, J. M. Haywood and S. R. Osborne of Met Office, Exeter were prepared as part of their official duties as employees of the UK Government. They are published with the permission of the Controller of Her Majesty's Stationery Office and the Queen's Printer for Scotland

observation period (SOP0) (Haywood *et al.*, 2008) and also coincided with the deployment of the Atmospheric Radiation Measurement (ARM) Mobile Facility (AMF) at Niamey (Miller and Slingo, 2007; McFarlane *et al.*, 2009). A common aim of these measurement campaigns was to improve the understanding of aerosols in West Africa, and their influence on the radiation budget and climate of the region (see Haywood *et al.*, 2008; Slingo *et al.*, 2008 and references therein).

Aircraft measurements during DABEX showed that the biomass-burning aerosol was strongly absorbing, with a single-scattering albedo of around 0.81 at 550 nm (Johnson *et al.*, 2008a). This compares with values of 0.85–0.90 measured during the Southern African Regional Science Initiative (SAFARI-2000) (Eck *et al.*, 2003; Haywood *et al.*, 2003a; Leahy *et al.*, 2007). In contrast, the dust aerosol was very weakly absorbing with single-scattering albedos of around 0.98 at 550 nm (Osborne *et al.*, 2008). AERONET retrievals from the Banizoumbou site (version 2 of the inversion algorithm) gave column-average single-scattering albedos in the range 0.81–0.92 but these were 0.03–0.08 lower than column-mean estimates from the aircraft *in situ* measurements (Osborne *et al.*, 2008). Interestingly, version 1 gave closer agreement with the aircraft single-scattering albedos.

Lidar and aircraft *in situ* measurements revealed an interesting vertical structure, with dust aerosol at low altitudes (typically below 2 km) and biomass-burning aerosol mixed with some dust aerosol in elevated layers between 2 and 5 km (Heese and Weigner, 2008; Johnson *et al.*, 2008b). Aircraft-observed size distributions in the biomass-burning layers were similar to those from SAFARI-2000 except that the concentration of coarse particles (e.g. radii >0.35 μm) was up to ten times higher, due to the mixing with dust. Comparisons of AERONET-retrieved size distribution and aircraft data gave mixed results during dusty conditions (Osborne *et al.*, 2008). Version 1 gave spuriously high concentrations of very fine particles (radii <0.1 μm), but this problem was corrected in version 2, as described by Dubovik *et al.* (2006). However, the relative proportions of coarse- and fine-mode volumes from AERONET version 2 still differed significantly from the aircraft observations during dust events. These differences were not fully reconciled by considering known errors in the aircraft optical measurements (e.g. assumptions on particle shape and refractive index).

One of the objectives of DABEX and AMMA-SOP0 was to assess the performance of satellite-based aerosol retrieval products over West Africa. Christopher *et al.* (2008) showed that Multi-angle Imaging SpectroRadiometer (MISR) AOD compared very well with AERONET stations over North Africa during 2005–2006. MISR AODs were therefore used to form empirical relationships between AOD and Aerosol Index (AI) from the Total Ozone Mapping Spectrometer (TOMS). This regression technique allows AOD to be estimated from TOMS AI, which has much better spatial–temporal coverage than MISR. AODs were also retrieved from the Moderate Resolution Imaging Spectroradiometer (MODIS) on board the National Aeronautics and Space Administration (NASA) Terra and Aqua satellites. Myhre *et al.* (2008) showed there was a good correspondence between MODIS and MISR in the January 2006 monthly-mean AOD patterns over West Africa. However, the standard MODIS algorithm (Remer *et al.*, 2005) was often unable to make retrievals over the bright surfaces surrounding and northwards of Niamey (13.3°N). A new MODIS algorithm called Deep Blue has shown success in retrieving AODs over bright desert surface (Hsu *et al.*, 2004, 2006), although there have not yet been any comparisons or validations during the DABEX/AMMA-SOP0 period.

A so-called 'golden-day' case-study occurred during DABEX on 19 January 2006. On this day clear skies were combined with high loadings of biomass-burning aerosol over the DABEX region. Nearby overpasses of NASA's Terra and Aqua satellites also provided excellent coverage from the MISR and MODIS instruments. The FAAM aircraft flew on the morning of 19 January making measurements of the vertical distribution of aerosols and their optical properties at a range of altitudes above Niamey (13.3°N, 2.1°E) and the AERONET site of Banizoumbou (13.5°N, 2.7°E) located just 50 km to the east of Niamey.

This paper compares the FAAM aircraft measurements against a variety of radiometric/remote-sensing measurements made within the Niamey and Banizoumbou region. These include the Banizoumbou AERONET sunphotometer, a hand-held Microtops sunphotometer operated at Niamey, MISR (from the Terra satellite), MODIS Deep Blue (from the Aqua satellite), and measurements made by the AMF at Niamey, including the Micro-Pulse Lidar (MPL), the Multi-Filter Rotating Shadow-band Radiometer (MFRSR) and the SKYRAD broadband radiometer system.

2. Data collection methods

2.1. Flight patterns

Figure 1 shows the flight track of the UK FAAM aircraft during flight number B159 on 19 January 2006. The plot only shows the track between 0925 and 1050 UTC when the aircraft flew a specific pattern of profiles and runs over Niamey and Banizoumbou. This pattern of profiles and runs is shown schematically in Figure 2. The pattern starts with a profile ascending from an altitude of 15 m above the runway at Niamey airport to 4.5 km. The aircraft then performed a series of four runs at altitudes of 3 km, 2.4 km, 1.8 km and 150 m, as shown in Figure 2. These runs were roughly aligned in the vertical following a southwest–northeast track over Niamey and Banizoumbou.

2.2. Aircraft *in situ* sampling

Aerosol size distributions were measured by the Particle Measuring Systems (PMS) Passive Cavity Aerosol

DOI: 10.1002/qj

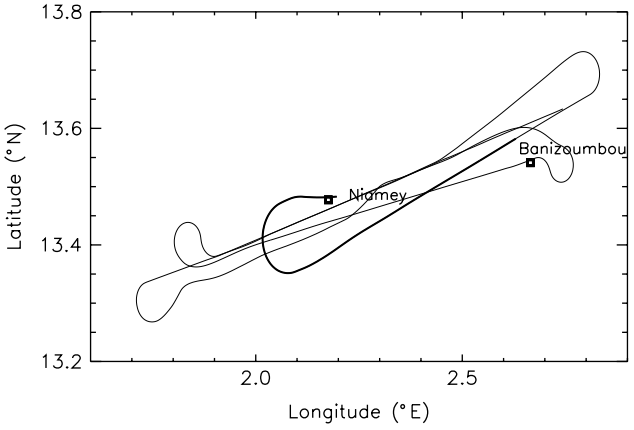

Figure 1. Track of the FAAM aircraft during the flight on 19 January 2006. The track during the profile is highlighted with a thicker line.

Spectrometer Probe 100X (PCASP), which sizes aerosols with radii in the range 0.05–1.5 μm. The PCASP is calibrated using latex spheres of known sizes that have a refractive index of $1.588 + 0.0i$. Corrections for refractive index have been applied to the PCASP size bin radii following the method of Liu and Daum (2000) (see Johnson *et al.*, 2008a for more details). The sizing algorithm of the PCASP instrument assumes spherical particles, whereas dust is known to exist in irregular shapes producing different scattering properties from spheres. Osborne *et al.* (2008) performed T-Matrix calculations using prolate cylinders and prolate spheroids to assess the likely sizing errors resulting from the spherical assumption. This showed typical sizing errors of around 10% for cylinders with an aspect ratio of 1.7 and smaller errors for spheroids with the same aspect ratio.

Aerosol scattering coefficients were measured at wavelengths of 450, 550 and 700 nm by a TSI 3563 nephelometer. The nephelometer data were corrected using Anderson and Ogren (1998) sub-micron corrections. The aerosol absorption coefficient was measured by a Radiance Research Particle Soot Absorption Photometer (PSAP), which operates at a wavelength of 567 nm. The PSAP absorption coefficient was corrected for errors in filter exposure area, air-flow rate, the influence of scattering by aerosols collected on the filter, and multiple scattering within the filter, following Bond *et al.* (1999). A small adjustment was made to convert the absorption coefficient from 567 nm to 550 nm – the central wavelength of the nephelometer. This adjustment was estimated using Mie calculations based on the aircraft size distributions (Johnson *et al.*, 2008a). No corrections are made for evaporation of water within the aerosol instruments because the ambient relative humidity was quite low (∼40%) and did not exceed 70% during the flight. At these low relative humidities the water content of the aerosol is expected to be small and have little impact on the scattering or absorption cross-sections of the aerosol.

2.3. Aircraft measurement of downwelling radiation

The total downwelling solar flux was measured by an Eppley pyranometer mounted on the top of the aircraft. This was fitted with a clear glass dome that transmitted radiation across the wavelength range of 0.3–3.0 μm. The pyranometer is calibrated annually by intercomparison with a transfer standard pyranometer.

The instrument mounting is pitched approximately 3° forward relative to the aircraft to partially offset for the 5–6° pitch of the aircraft during straight and level flight. Although corrections are made for the pitch and roll of the aircraft during flight, uncertainties of ±0.5° in the pitch and roll of the instrument mounting, relative to the aircraft, may have contributed to errors of ±2% in the measured flux (depending on solar zenith angle and aircraft heading). When combined with basic instrumental uncertainty we consider the aircraft

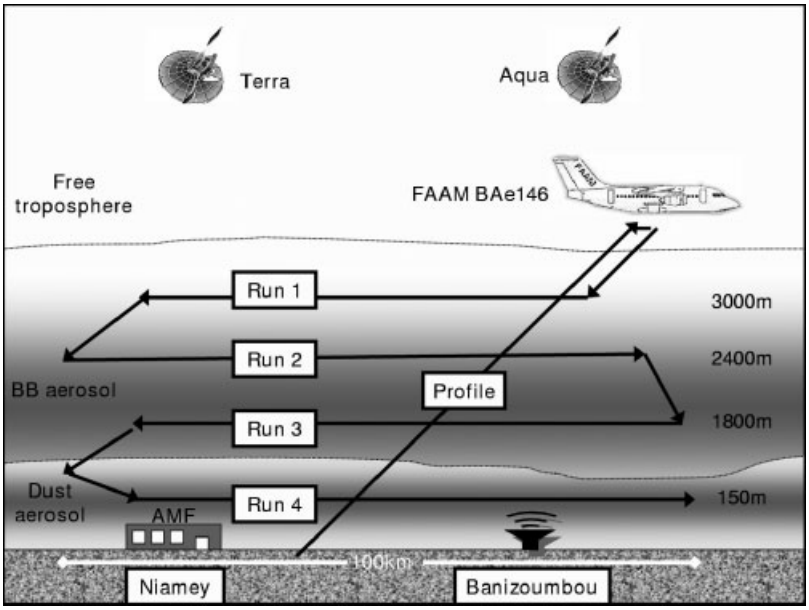

Figure 2. Schematic of the measurement platforms used in this case-study and the aircraft flight pattern during the flight on 19 January 2006.

DOI: 10.1002/qj

pyranometer measurements to have an uncertainty of around 3%.

2.4. Radiative transfer modelling

The Edwards and Slingo radiative transfer model (Edwards and Slingo, 1996) was used to calculate radiative fluxes across the solar spectrum. A high spectral resolution version of the model was used with 220 spectral bands covering wavelengths from 200 nm to 10 μm. The model calculated radiance using a series of 21 spherical harmonics and integrated over angles to compute vertical fluxes.

Profiles of atmospheric temperature and humidity were derived via a combination of aircraft data (for altitudes up to 4 km) and sonde data (for altitudes above 4 km). The sonde data were from a launch made at 1041 UTC on 19 January 2006 at the AMF in Niamey. The profile of ozone was derived from the aircraft data for altitudes up to 4 km, and from climatological data (McClatchey *et al.*, 1972) for altitudes above 4 km. The surface albedo was estimated as a function of wavelength using measurements of upwelling and downwelling solar radiation from the FAAM aircraft during run 4, approximately 150 m above the ground. These suggested a broadband average albedo of 0.28 but with a strong decrease in albedo with decreasing wavelength (strong absorption in the blue and ultraviolet, as expected for orange-brown coloured ground). The spectral variation of surface albedo was estimated from nadir radiance measurements making the assumption that the spectral dependence of the albedo was invariant with viewing or illumination angle. Although this assumption may not hold well for certain surfaces, we consider it better than applying the broadband albedo to all wavelengths (i.e. assuming a grey surface) when visual observations were of an orange-brown landscape.

The model included representations for both dust and biomass-burning aerosol and treated each species separately (i.e. assuming an external mixture, which is consistent with the observations from Formenti *et al.* (2008) and Chou *et al.* (2008)). Aerosol optical properties were derived from Mie calculations based on log-normal fits to the aircraft PCASP data from the FAAM aircraft profile. The PCASP data were also supplemented with size distribution retrievals from the Banizoumbou AERONET to enable a continuation of the size distribution to sizes greater than 1.5 μm radius; the size limit of the PCASP (see section 6). Two log-normals were used to capture the fine mode (radii 0.05–0.35 μm) and three log-normals were used to capture the coarse mode (radii 0.35–10 μm). Based on detailed examination of aircraft data in Johnson *et al.* (2008a), we believe the fine mode to be dominated by biomass-burning aerosol and the coarse mode to be dominated by dust. The 0.35 μm cut-off radius between the fine and coarse mode corresponded to a local minimum (inflexion point) in volume size distributions (see Fig. 8b of Johnson *et al.*, 2008a). For the purposes of modelling we assume all particles larger than 0.35 μm to be dust and all particles smaller than 0.35 μm to be biomass-burning aerosol. In reality some of the fine particles are likely to be dust, so we also ran a sensitivity test assuming that 25% of the fine mode was dust (the remaining 75% being biomass-burning aerosol).

The biomass-burning aerosol was assumed to be a mixture of organics and soot (black carbon) with a black carbon volume fraction of 6%. Refractive indices for the organics and soot were taken from WCP (1986). This gave the biomass-burning aerosol a refractive index of $1.54 + 0.045\mathrm{i}$ and single-scattering albedo of 0.81 at 550 nm, as in Johnson *et al.* (2008a). This led to good agreement with the observed single-scattering albedo of 0.82 ± 0.04 observed during run 1 that was strongly dominated by biomass-burning aerosol. The refractive index of the dust aerosol was based on data from Balkanski *et al.* (2007), using the low (0.9%) haematite model. This gave the dust a refractive index of $1.512 + 0.00092\mathrm{i}$ across most of the solar spectrum (300–2000 nm) and a single-scattering albedo of 0.98 at 550 nm, which agreed well with the single-scattering albedo of 0.98 ± 0.02 observed in the low-level dust layer during run 4. This is a slight adjustment from Osborne *et al.* (2008) who suggest a refractive index of $1.53 + 0.0004\mathrm{i}$ and single-scattering albedo of 0.99 from different flights targeting moderate to strong dust events during DABEX. The vertical distribution of aerosol was scaled to the vertical distribution of aerosol scattering measured by the nephelometer green channel. Absolute values of aerosol mixing ratio were scaled to the AOD from the Microtops sunphotometer to faithfully capture the temporal variation of AOD through the day. The outcome of the size distribution fitting and refractive index assumptions was that 65% of the AOD in the model was from the fine mode (biomass-burning aerosol) and 35% was from the coarse mode (dust aerosol).

2.5. ARM Mobile Facility

The ARM Mobile Facility (AMF) was stationed at Niamey Airport throughout 2006 (Miller and Slingo, 2007; Slingo *et al.*, 2008). AODs were estimated by the MFRSR which measures solar irradiance at six wavelengths (415, 500, 615, 673, 870 and 940 nm). Direct normal irradiance is derived from the four shadow-band measurements made at each data point (Harrison and Michalsky, 1994). The MFRSR irradiances were calibrated by multiple Langley regressions throughout the deployment, and then AOD at each measurement wavelength was derived from the calibrated direct normal irradiance. The AOD at 550 nm is calculated using the Ångström exponent derived from the AODs at 415 nm and 673 nm, for consistency with the AERONET processing described below. A Micro-Pulse Lidar (MPL) was used to derive profiles of aerosol extinction coefficient. The backscatter-to-extinction ratio was assumed to be constant with height and was estimated using AODs from the MFRSR. The preferred method for measuring total downwelling short-wave flux is to combine the direct and diffuse beam measurements from two separate

DOI: 10.1002/qj

instruments. However, initial analysis of the radiometers at the AMF sites indicates a potential problem in the solar tracker during January, which may affect the direct and diffuse beam measurements. Thus, while this issue is under investigation, we use the total downwelling short-wave radiation measured by an unshaded Eppley pyranometer as part of ARM's Sky Radiation (SKYRAD) system. This was corrected for thermal offsets following the procedure of Younkin and Long (2003) and using regression coefficients obtained from the full year of radiometer data at Niamey. The fluxes from the corrected unshaded pyranometer measurements differ from the sum of the diffuse and direct beams by <8 W/m^2. Further details on the AMF instruments are available at http://www.arm.gov/sites/amf.stm.

2.6. AERONET and Microtops sunphotometers

AERONET data from the Banizoumbou site were obtained from http://aeronet.gsfc.nasa.gov. Direct sun measurements were used to estimate AODs. These were interpolated to a wavelength of 550 nm using the data at 438 nm and 675 nm and assuming a constant Ångström exponent across that wavelength range. Ångström exponents were calculated from the AODs at 438 nm and 675 nm. Almucantar scans were used in conjunction with the version 1 and version 2 inversion algorithms to estimate aerosol size distribution, complex refractive index and aerosol optical properties. The version 2 algorithm includes a representation for particle asphericity via randomly orientated prolate and oblate spheroids (Dubovik *et al.*, 2006). The version 1 algorithm used in this study assumed spherical particles (Dubovik and King, 2000). Single-scattering albedos and asymmetry parameters from these inversions were interpolated assuming a logarithmic interpolation. The Microtops II is a handheld sunphotometer, manufactured by Solar Light. This measured AOD at wavelengths of 380, 440, 675, 936 and 1020 nm by measuring the intensity of the direct solar beam. Comparisons with AERONET sunphotometers showed Microtops II AODs to be accurate to within ± 0.02 when operated correctly in cloud-free conditions (Ichoku *et al.*, 2002). As with AERONET, the AOD at 550 nm was estimated via logarithmic interpolation.

2.7. Satellite data

The MISR has four spectral bands (446, 558, 672 and 866 nm) and nine cameras at different angles. The swath width is 360 km and global coverage is achieved after nine days. The unique multiple viewing geometries of MISR enable a greater ability to distinguish between the effects of aerosol scattering and surface reflectance on upwelling radiation at the top of the atmosphere. MISR therefore compares well with AERONET AODs over deserts, despite their bright surfaces (Christopher and Wang, 2004; Martonchik *et al.*, 2004; Christopher *et al.*, 2008). A global comparison of MISR and AERONET AODs shows that overall, 63% of the MISR-retrieved AOD values fall within 0.05 or 20% of AERONET AODs, and about 40% are within 0.03 or 10% (Kahn *et al.*, 2005). The MISR swath covered the Niamey and Banizoumbou region on 19 January 2006, due to an almost overhead passage of the Terra satellite. We use the MISR L2 aerosol product (MIL2ASAE) for AOD at 558 nm, which is a validated product. We also use retrievals of single-scattering albedo, asymmetry parameter, and the fraction of optical depth attributed to the small (<0.35 μm radius), medium (0.35 to 0.70 μm radius), and large (>0.70 μm radius) size categories. These are considered beta-quality products and validation of these products by the MISR science team are ongoing.

The MODIS on NASA's Terra and Aqua satellites has a wide swath of about 2400 km and provides near-global coverage on a daily basis. The MODIS collection 5 operational algorithm provides AOD retrievals over global oceans and dark land areas. A complementary algorithm called MODIS Deep Blue provides AODs over bright surfaces such as deserts. It matches the measured 412, 470 and 650 nm channel reflectances with theoretical radiative transfer calculations to retrieve AOD. Comparisons between the Deep Blue and AERONET AODs are generally within 20–30% of each other (Hsu *et al.*, 2006). We used collection 5.1 of the Deep Blue product over the area of interest. Because Deep Blue data have currently only been processed for the AQUA platform, the comparisons that we present use composite standard/Deep Blue retrievals from AQUA.

To derive the MISR and MODIS Deep Blue AODs over Banizoumbou and Niamey we took a mean of all valid retrievals within a $0.5^\circ \times 0.5^\circ$ box centred over those locations. The standard deviation of AOD within these boxes was taken as an indication of the uncertainty of the mean AOD value (see section 4). The same averaging process was applied to derive MISR single-scattering albedos over Banizoumbou and Niamey.

3. Vertical distribution of aerosol and thermodynamic variables

Figure 3(a) shows the vertical profile of aerosol scattering coefficient measured by the nephelometer during the aircraft profile (0925–0940 UTC). This suggests a shallow layer of dust aerosol from the surface to about 1 km and a deep layer of biomass-burning aerosol and dust from 1 to 3 km. The variation of scattering coefficient with wavelength is very small in the lower layer indicating dominance by coarse particles, which are likely to be dust. The scattering coefficient is stronger at the shorter wavelengths in the upper aerosol layer indicating the presence of fine particles, which we assume to be biomass-burning aerosol. Evidence from the PCASP suggested these were also mixed with dust in the upper layer (Johnson *et al.*, 2008a). The top of each aerosol layer is marked by a small increase in potential temperature and a change in the dew-point temperature (Figure 3(b)). The biomass-burning layer has a higher potential temperature and is more humid

DOI: 10.1002/qj

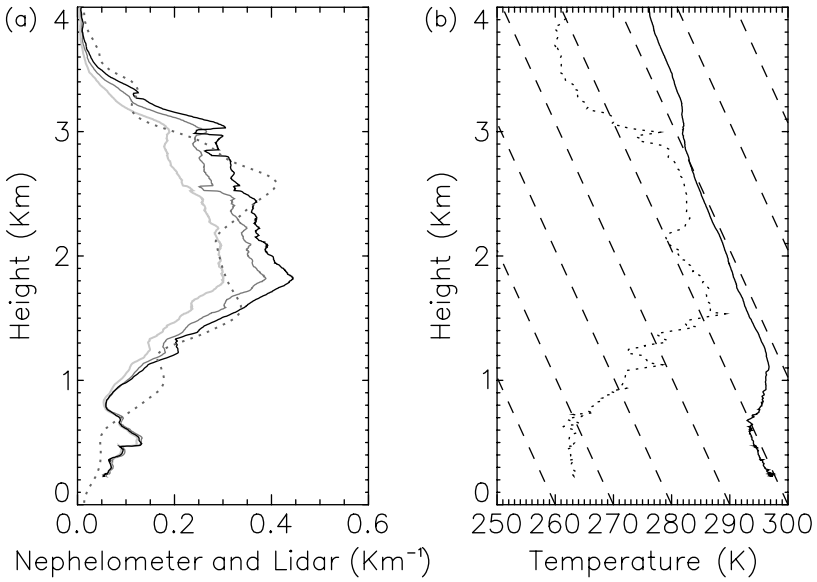

Figure 3. (a) Vertical profiles of nephelometer scattering coefficients (km^{-1}) from the FAAM aircraft at wavelengths of 450 (black line), 550 (dark-grey line) and 700 nm (light-grey line) and lidar extinction coefficient (km^{-1}) at 523 nm from the AMF MPL (dark-grey dotted line). (b) Temperature (solid line) and dew-point temperature (dotted line) from the FAAM aircraft, with lines of constant potential temperature (dashed lines) at intervals of 10K.

than the dry dusty layer near the surface. The dust layer originated from the north (the Sahara Desert) whereas the biomass-burning aerosol layer originated from the southwest, as shown by back-trajectory modelling in Figure 7 of Johnson *et al.* (2008a). This kind of vertical distribution and atmospheric flow pattern was typical of DABEX, as illustrated in Haywood *et al.* (2008).

The vertical distribution of aerosol was also retrieved by the MPL lidar at the AMF in Niamey. The lidar extinction coefficient (at 523 nm) is shown in Figure 4 as a function of time and height during 19 January 2006. This shows a broad layer of aerosol between 1 and 3 km that persists throughout the day but becomes thinner and more diffuse in the afternoon. The lidar extinction profile averaged over 0900–1000 UTC is shown in Figure 3(a) alongside the nephelometer data from the aircraft profile (made at 0925–0940 UTC). The lidar shows a broad agreement with the aircraft nephelometer profile although some differences are apparent, particularly in the profile below 1 km. The lidar extinction peaks at around 2.5 km, as shown in both Figures 3(a) and 4, whereas the nephelometer scattering peaks at around 1.8 km. These slight differences in profile may be due to the spatial variability within the aerosol layer that is encountered during the long slant path of the aircraft profile. Inhomogeneity of the aerosol field is reflected to some degree by the temporal variability in lidar extinction data. Furthermore, a direct comparison of absolute values can not be made since the nephelometer measures only scattering and not extinction, plus there is a small difference in wavelength between the nephelometer green channel (550 nm) and the lidar (523 nm). The MPL also assumed the backscatter-to-extinction to be constant with height, neglecting any vertical variability in aerosol scattering properties.

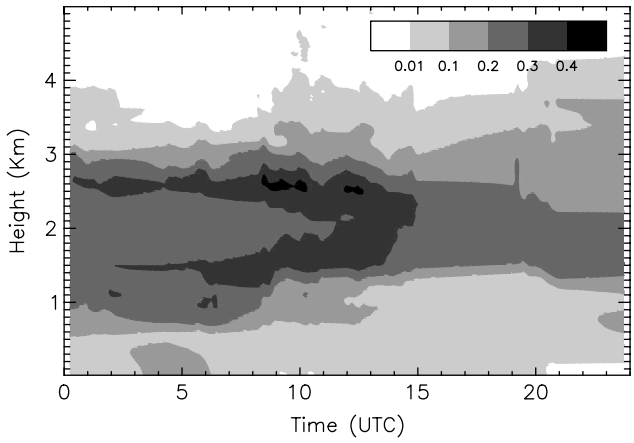

Figure 4. MPL lidar-derived extinction coefficient (km^{-1}) at 523 nm from the AMF at Niamey Airport during 19 January 2006.

4. Aerosol optical depths

Figures 5 and 6 show the regional patterns of AOD on 19 January 2006 from the MODIS and MISR satellite instruments. The MODIS figure combines standard retrievals made over dark surfaces to the south of Niamey and Deep Blue algorithm retrievals over brighter surfaces north of around 13°N. The AODs in the Niamey–Banizoumbou region were from the Deep Blue algorithm. The Figures show high AODs of 0.5–0.8 in the case-study region around Banizoumbou and Niamey but the MISR AODs are 0.1–0.2 higher than MODIS AODs. MODIS also shows some very low AODs of 0.1–0.3 to the south of Niamey (e.g. 11°N, 2°E) whereas MISR generally does not have AODs below 0.3 in that region. In general the spatial patterns of AOD from MODIS and MISR are not that well matched. These differences may be partly explained by the three-hour

DOI: 10.1002/qj

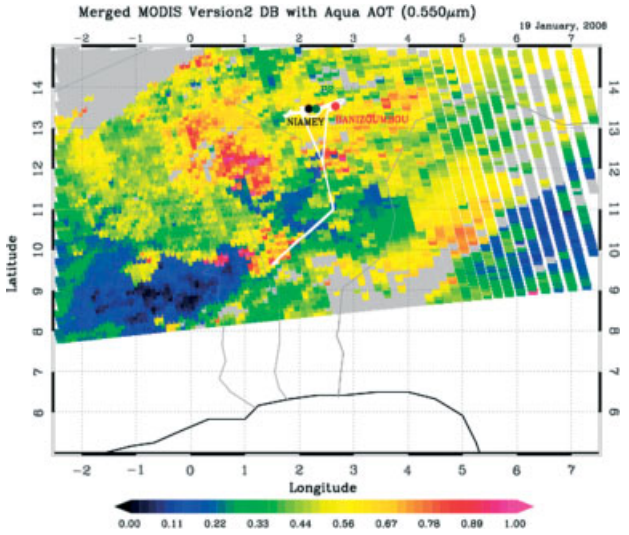

Figure 5. AOD at 550 nm, combined from MODIS collection 5 and MODIS Deep Blue collection 5.1 from the Aqua satellite overpass at 1330 UTC on 19 January 2006. Light-grey indicates areas where no retrieval was possible, e.g. due to cloud.

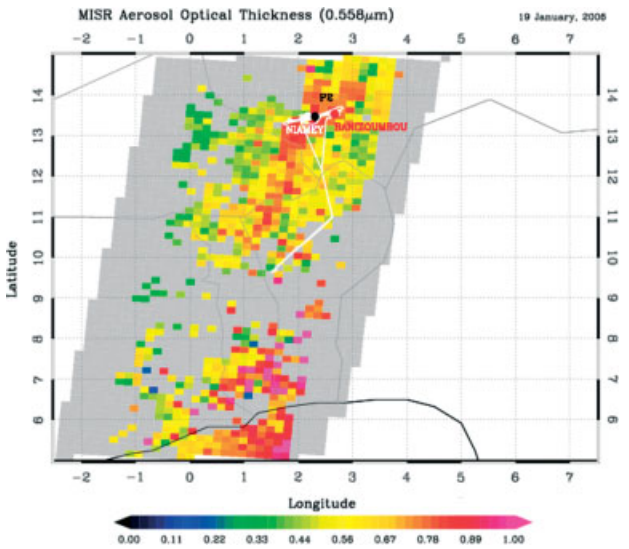

Figure 6. MISR AOD at 558 nm from Terra Satellite at 1030 UTC on 19 January 2006. Light-grey indicates areas where no retrieval was possible, e.g. due to cloud.

time difference between the satellite overpasses (1030 UTC for MISR on Terra, 1330 UTC for MODIS on Aqua). The sun photometer measurements suggest a drop in AOD of 0.05–0.07 over that time period in the Niamey–Banizoumbou region; a 10% change, which does not fully account for the differences in the two images. Differences in retrieval performance therefore seem likely. The coverage by MISR is more limited due to the narrow swath of the instrument but also sparser, perhaps due to more selective quality control criteria.

Figure 7 compares AODs at 550 nm from various instruments in the Banizoumbou and Niamey area during 19 January 2006. AODs are also listed in Table I, along with uncertainty estimates. Where measurements were not available at 550 nm, measurements at nearby

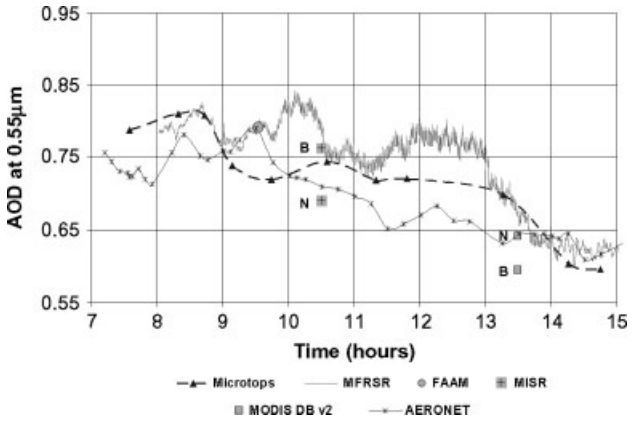

Figure 7. AODs versus time on 19 January 2006 from various sources including: Banizoumbou AERONET, Microtops at Niamey, MFRSR at Niamey, FAAM aircraft, MFRSR, and the MISR and MODIS Deep Blue satellite retrievals co-located with Banizoumbou (B) and Niamey (N).

wavelengths were interpolated to 550 nm using logarithmic interpolation. The AERONET, Microtops and MFRSR measurements suggest a gradual decrease of AOD from around 0.75 in the morning (0730–1000 UTC) to 0.60 by 1500 UTC. This occurs in parallel to a gradual drop in the vertical thickness of the aerosol layer between 1 and 3 km, as shown by the MPL measurements (Figure 4). The AERONET and Microtops sunphotometer AODs generally agree to within 0.07 and there are no obvious systematic differences between the two instruments. The differences in AOD between AERONET and Microtops are probably due to differences in the location of the instruments, since instrumental uncertainties in sunphotometer AODs are not expected to be more than 0.02 (Eck *et al.*, 1999; Ichoku *et al.*, 2002). Figures 5 and 6 show a fair degree of variability in AOD, which may be due to horizontal variability of the AOD since the Banizoumbou AERONET site was approximately 50 km to the northeast of Niamey where the Microtops measurements were made. The MFRSR was located at Niamey Airport, just 5 km from the city location where the Microtops was operated. Therefore, the MFRSR ought to agree closely with Microtops but there are significant deviations, especially during mid-morning (1000 UTC) when the MFRSR AOD is up to 0.1 higher than Microtops.

The MFRSR estimates AOD from the ratio of diffuse to direct solar radiation using a shadow-band to block the sun for the diffuse sky measurement. The solar aureole contribution to the blocked measurement is estimated by taking two sideband measurements. For most aerosol conditions, errors in AOD due to the underestimate of the solar aureole contribution are negligible; however, they become more significant for coarse aerosols such as dust with effective radius >1 μm, due to the larger forward scattering contributions (Alexandrov *et al.*, 2007). Comparisons to a co-located sun photometer at Niamey during the latter half of 2006 indicate that the MFRSR underestimates AOD by 15–20%, due to forward scattering by the large dust particles. A correction for the forward scattering has been implemented for the AOD

DOI: 10.1002/qj

Table I. AODs and aerosol optical properties at 550 nm on 19 January 2006.

Data source	Location[a]	Time (UTC)	AOD	Ångström exp.	ω	k_{ext}	g
FAAM:							
Run 1 (3km)	B/N	0947–0956	–	1.13 ± 0.12	0.82 ± 0.05	1.78	0.66
Run 2 (2.4km)	B/N	0949–1012	–	0.83 ± 0.12	0.86 ± 0.04	1.27	0.67
Run 3 (1.8km)	B/N	1014–1028	–	0.82 ± 0.12	0.88 ± 0.04	1.23	0.68
Run 4 (150m)	B/N	1037–1049	–	-0.06 ± 0.11	0.98 ± 0.02	0.48	0.73
Column-mean	B/N	0925–1049	0.79 ± 0.12	0.84 ± 0.12	0.87 ± 0.04	1.13	0.68
AERONET v2	B	1030	0.71 ± 0.02	0.90 ± 0.06	0.85 ± 0.03	–	0.70
AERONET v1	B	1030	0.71 ± 0.02	0.90 ± 0.06	0.91 ± 0.03	–	0.66
Microtops	N	1035	0.75 ± 0.02	0.82 ± 0.06	–	–	–
MFRSR	N	1030	0.80 ± 0.07	0.84 ± 0.03	–	–	–
MISR	B	1030	0.76 ± 0.07	0.49 ± 0.13	0.94 ± 0.01	–	–
MISR	N	1030	0.69 ± 0.2	0.82 ± 0.35	0.94 ± 0.01	–	–
MODIS DB	B	1330	0.59 ± 0.06	–	–	–	–
MODIS DB	N	1330	0.64 ± 0.06	–	–	–	–

[a] Location B refers to Banizoumbou, location N refers to Niamey, and B/N indicates that the measurements were in the general region of B and N (see Figure 1).

retrievals (Connor Flynn, personal communication) and is now available in the ARM archive. The corrected AOD estimates are shown in Figure 7 and Table I. It is not clear why the MFRSR and Microtops AODs agree during some time periods and differ during other periods of the day. There was no evidence for a change in the relative abundance of coarse particles between 0900 and 1030 UTC; the column-mean Ångström exponent from Microtops and AERONET varied little during the morning, with values ranging from 0.8 to 0.9 (estimated from AODs at 440 and 675 nm).

The FAAM AOD estimate was calculated by integrating the aerosol scattering profile, shown in Figure 3, over height and adding a contribution for aerosol absorption based on the column-average single-scattering albedo (0.87) estimated from the PSAP and nephelometer data during the four runs (see section 5). This method gave an AOD of 0.79 at 550 nm, as shown in Figure 7 and listed in Table I. Based on the instrumental uncertainties with the nephelometer and PSAP we estimate an uncertainty of 15%, or ± 0.12. At the time of the profile (0925–0945 UTC), Microtops indicated an AOD of 0.72 and AERONET indicated an AOD of 0.74. Thus the FAAM AOD estimate is no more than 10% above the sunphotometer AODs, which is well within the instrumental uncertainty. It is also important to recognise that the aircraft covered a horizontal path of about 100 km during the profile (see the bold line in Figure 1) so the FAAM AOD estimate is not a true column measurement. On four other flights during DABEX, FAAM AODs were also within 10% of AOD estimates from Banizoumbou (Johnson *et al.*, 2008b). The comparison here gives us confidence that the aircraft scattering and absorption measurements are of reasonable magnitude, and are not grossly affected by problems with sampling efficiency (as had been a concern when sampling dust aerosol during previous measurement campaigns with the Met Office C-130 aircraft (Haywood *et al.*, 2003b)).

The MISR and MODIS Deep Blue AOD retrievals at Banizoumbou and Niamey are also shown in Figure 7 and listed in Table I. These satellite AODs are within 10% of the AERONET and Microtops sunphotometer measurements, which is very encouraging given the inherent difficulty of retrieving AOD from satellites over bright land surfaces. The true level of uncertainty in these satellite AODs is difficult to estimate. Table I gives the uncertainties as the standard deviation of the AOD retrieved within the $0.5^\circ \times 0.5^\circ$ averaging box centred over the Banizoumbou and Niamey sites. These are about 0.05 for MODIS and 0.07–0.2 for MISR. Such scatter or variability can be expected, given uncertainties in surface reflectance and the spatial variability of the aerosol field. However, the standard deviation for MISR in the box over Niamey (0.2) does seem excessive compared to the typical differences between measurements at Niamey and Banizoumbou AOD, which are 50 km apart (about the size of the averaging boxes of the satellite data). The fact that MODIS gives lower AODs than MISR is consistent with the downward trend of AODs during the day, as shown by the AERONET, Microtops and MFRSR data in Figure 7.

5. Aerosol optical properties

Table I shows AODs and aerosol optical properties derived from the FAAM aircraft, the AERONET and Microtops sunphotometers, the MFRSR, and the MODIS and MISR satellite retrievals. Aircraft measurements were averaged along runs 1–4 and a column average was estimated combining data from all four runs. The weighting for the column-average optical properties was based on the optical depth of the layer represented by each run. The aircraft-derived Ångström exponent was calculated from the 450 and 700 nm scattering coefficients from the nephelometer. The Ångström exponent increases with

DOI: 10.1002/qj

height indicating an increasing importance of fine particles (i.e. biomass-burning aerosol) at higher altitude, as also reflected in the nephelometer profile of Figure 3(a). The column-mean Ångström exponent of 0.84 is about halfway between the value in the dust layer (near zero) and the value of 1.7 that was estimated for the biomass-burning aerosol component in Johnson *et al.* (2008a). Mie calculations showed that there was a roughly linear relationship between the Ångström exponent and the proportion of extinction associated with biomass-burning aerosol (Johnson *et al.*, 2008b), assuming mineral dust and biomass burning were the only sources of aerosol in the atmosphere. Therefore, the Ångström exponent of 0.84 in this regression would suggest that the dust and biomass-burning aerosol contributed equally ($50 \pm 7\%$) to the AOD at 550 nm. However, the Mie calculations performed as part of this study (see section 2.4) suggested a more dominant role for the biomass-burning aerosol with such particles accounting for 65% of the AOD at 550 nm. This division between dust and biomass-burning aerosol was based on an interpretation of the PCASP data rather than the Ångström exponent from the nephelometer. This may indicate a weakness in the assumption, employed in section 2.4, that all particles smaller than 0.35 μm radius are associated with biomass-burning aerosol. If we assumed instead that 25% of the fine particle AOD was actually from dust then the two methods fall into agreement with a 50/50 split between the dust and biomass-burning AOD.

The single-scattering albedo measured by the nephelometer and PSAP on the aircraft varied from 0.98 ± 0.02 in the dust layer (run 4, at an altitude of 150 m), to 0.82 ± 0.04 in the upper part of the biomass-burning aerosol layer (run 1, at an altitude of 3 km). On runs 2 and 3 at intermediate altitudes the single-scattering albedo was 0.86 ± 0.03 and 0.88 ± 0.03, respectively. The column-mean value was estimated as 0.87 ± 0.03. These values were fairly typical of the FAAM measurements during DABEX (Johnson *et al.*, 2008a; Osborne *et al.*, 2008) and the decrease of single-scattering albedo with height was linked to the diminishing influence of dust and growing influence of biomass-burning aerosol at higher altitudes.

The aircraft-based measurements of specific extinction coefficient (k_{ext}) and asymmetry parameter (g) were estimated from Mie calculations (at 550 nm) using the PCASP size distributions, extended into the coarse range (radii >1.5 μm) using a log-normal fit to the AERONET data, and refractive indices as outlined in section 2.4. The specific extinction coefficient increases with height and the asymmetry parameter decreases slightly with height, as expected due to the increasing dominance of the biomass-burning aerosol with height. Furthermore, by employing Mie calculations we assume all particles to be spherical. T-Matrix calculations reported in Osborne *et al.* (2008) showed that particle shape made negligible difference to the single-scattering albedo and asymmetry parameter but led to. errors of up to 21% in mass extinction coefficient for pure dust size distributions. Errors in this study are likely to be less, particularly at the higher altitudes where the dust is less dominant in the aerosol mixture.

The remote-sensing measurements also provide information on aerosol optical properties. Ångström exponents from the sunphotometers, MFRSR and aircraft seem fairly consistent given expected instrumental errors (see Table I) and the spatial–temporal variability of the aerosol field. Time series of AERONET and Microtops Ångström exponents showed variation of no more than 0.05 during the main period of interest (0900–1100 UTC) (result not shown). The MISR Ångström exponent agrees well with other estimates of Ångström exponent for the retrieval over Niamey (0.82) but is below the other estimates for the retrieval over Banizoumbou (0.49). The discrepancy is most likely due to limited choices of aerosol types in the MISR aerosol retrieval algorithm. In particular, the lack of aerosol mixtures containing both dust and absorbing spherical particles in the standard MISR algorithm (version 22) can be a contributing factor in this case (Kahn *et al.*, 2005, 2009; Chen *et al.*, 2008). The standard deviation of MISR Ångström exponent was quite large (0.13 over Banizoumbou, 0.35 over Niamey) indicating variability in the aerosol mixtures picked by the algorithm.

The single-scattering albedo from AERONET version 2 (0.85) is slightly lower than the column-mean value from the FAAM aircraft (0.87), although the difference is well within the uncertainty range (± 0.03 for each instrument). The version 1 AERONET retrieval gives a much higher single scattering albedo of 0.91, which does not seem consistent with the aircraft observations. In comparisons from other DABEX flights, version 2 of the Banizoumbou AERONET retrieval gave single-scattering albedos that were 0.03–0.08 lower than column-mean values from the FAAM aircraft (Osborne *et al.*, 2008), whereas version 1 values were higher and in good agreement with the aircraft. It is possible that the version 1 algorithm retrieves single-scattering albedo more accurately for dusty conditions, whereas version 2 performs better in this case because the aerosol column was more strongly influenced by biomass burning than dust. The MFRSR gives a higher estimate of single-scattering albedo (0.90), although this is not inconsistent with AERONET or FAAM, given the expected uncertainty of ± 0.04 (from Kassianov *et al.*, 2007). The FAAM values of asymmetry parameter (0.68) compare well to AERONET values of 0.66 and 0.70 for versions 1 and 2, respectively. The MISR single-scattering albedo (0.94 ± 0.01) is substantially higher than aircraft or AERONET values, which again is likely due to limitations of the MISR algorithm mixture table, as noted above.

6. Aerosol size distributions

Figure 8 compares the size distribution from the FAAM aircraft PCASP instrument against retrieved size distributions from AERONET. The PCASP size distribution is a column average using data from the profile. The

DOI: 10.1002/qj

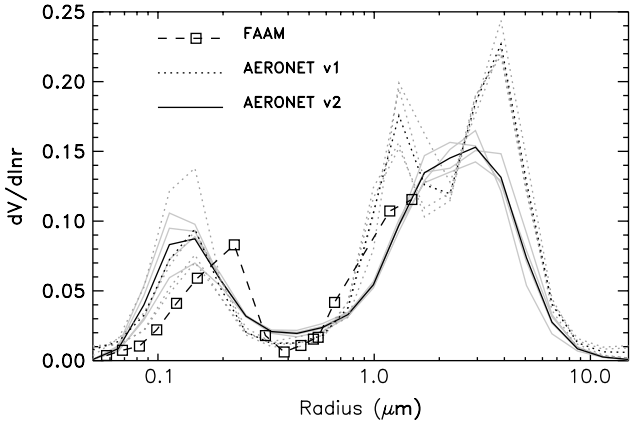

Figure 8. Aerosol size distributions from the FAAM aircraft PCASP instrument (squares and dashed line) and Banizoumbou AERONET retrievals (dotted lines for version 1, solid lines for version 2) during 19 January 2006. The darker lines show the daily mean AERONET retrievals. Data is normalized by total volume.

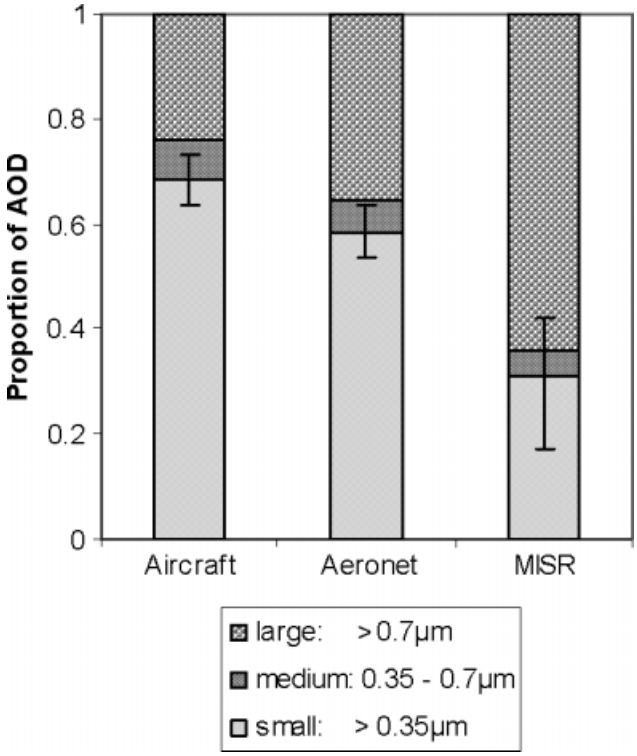

Figure 9. AOD contributions from small, medium and large aerosols, derived from the FAAM aircraft PCASP, Banizoumbou AERONET retrievals and MISR retrieval co-located with Banizoumbou. The error bars shows the uncertainty in the AOD contribution from the large size range. The uncertainties in the medium size range were comparatively small and the uncertainties in the fine size range approximately matched the uncertainties of the large size range.

figure shows data from both version 1 (Dubovik and King, 2000) and version 2 (Dubovik *et al.*, 2006) of the inversion algorithm. The daily mean retrievals are shown, as well as four individual retrievals made on the morning of 19 January between 0730 and 0900 UTC. There are significant discrepancies between the PCASP and AERONET retrievals that may reflect difficulties in making optical measurements (see section 2.2) and/or uncertainties associated with retrieval methods. However, there is agreement in the overall pattern of the distributions. Both show a fine mode from 0.05 to 0.4 μm and a coarse mode starting from about 0.75 μm upwards. Unfortunately the PCASP does not measure aerosols larger than 1.5 μm in radius and, owing to difficulties with other instruments, no aircraft data are available for the larger-sized aerosols. However, the available PCASP data do indicate a coarse mode with a similar magnitude to AERONET and a peak at sizes of 1.5 μm or greater. In general, the shape of the retrieved size distribution does not change much between individual AERONET retrievals and the corresponding daily mean, but there are significant differences between versions 1 and 2. Version 1 produces a double peak structure in the coarse size range with maxima at sizes of 1.5 and 4 μm. Version 2 produces a broader peak with a maximum at 3 μm. It is not clear from these comparisons which version is more realistic or reliable, although previous studies have shown clear improvements between version 1 and version 2 in dusty conditions (e.g. Osborne *et al.*, 2008).

The MISR retrieval splits total AOD into three size categories: small ($r < 0.35$ μm), medium (0.35–0.7 μm), and large ($r > 0.7$ μm). Figure 9 shows the breakdown of the AOD into these categories for the retrieval over Banizoumbou. A similar breakdown has been performed for the aircraft and AERONET data. This involved running Mie calculations with the aircraft and AERONET volume distributions and the refractive index assumptions from section 2.4. The aircraft shows a much lower contribution from the large particle category because particles greater than 1.6 μm were not measured by the aircraft PCASP. Since the AERONET size distribution covers a much wider size range (Figure 8) it is a better source of data for comparison against MISR. The MISR data shows a substantially larger proportion of the AOD coming from the large particle category. This is suggestive of a stronger contribution from dust-like aerosol in the retrieval model. This is consistent with the anomalously low Ångström exponent given in Table I and probably reflects limitations of the MISR algorithm mixture table, as discussed in section 5.

7. Short-wave radiative fluxes

The AMF observations show a smooth symmetric curve for most of the day, consistent with cloud-free conditions. The main deviations from this curve are in the afternoon (1530–1730 UTC), indicating some cloud cover. The FAAM observations are from run 4 that was made at 150 m above ground level past Niamey and Banizoumbou (see time period 1035–1045 UTC in Figure 10). The FAAM observations are about 20 W m^{-2} lower than those from the AMF at the beginning of the run and then in good agreement with the AMF at the end of the run, as shown by the inset of Figure 10. This variability along the aircraft run may be attributed to variability of the aerosol column above the aircraft, since the aircraft travelled roughly 80 km during the run. At the time that

DOI: 10.1002/qj

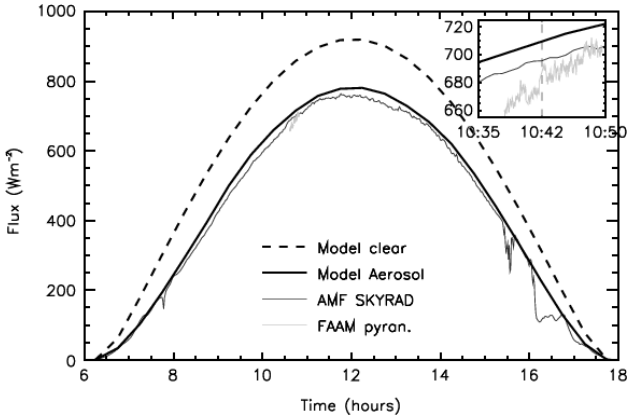

Figure 10. Total solar flux as a function of time on 19 January 2006 from the AMF SKYRAD system (dark-grey line), the FAAM pyranometer during run 4 (light-grey line), and radiative transfer modelling either including aerosol (black solid line) or assuming no aerosol (black dashed line). Inset focuses on the time period 1035–1050 UTC when FAAM run 4 measurements were made. The aircraft was closest to Niamey at 1042 UTC, as indicated by the grey dashed line.

the aircraft flew past Niamey (1042 UTC) the aircraft measurements are about the same as the values from the AMF, which shows a good agreement considering the expected uncertainty of around 3% in the FAAM pyranometer measurements. The difference in altitude between the aircraft and the AMF (approximately 150 m) is not expected to influence the comparison by more than 5 W m^{-2} since the aerosol concentration was quite low in the lowest 150 m of the atmosphere, as shown by the aerosol scattering profile in Figure 3(a).

The radiative transfer modelling is shown for calculations with and without aerosols (solid and dashed lines, respectively, in Figure 10). The model's aerosol optical properties and their vertical distribution were based on the aircraft observations from the profile and the runs 1–4 during the period 0925–1050 UTC. However, because there were changes in AOD during the day (Figure 7), the aerosol mass mixing ratios in the model have been scaled so that the AOD in the model follows that observed by the Microtops sunphotometer at Niamey. The model gives a slightly higher flux than the observations through most of the day. During the middle part of the day (1000–1400 UTC) this difference averaged 20 W m^{-2} (2.8% of the observed flux) but reached 30 W m^{-2} around 1300 UTC. More abrupt deviations also occur later in the afternoon (e.g. 1530 UTC) but these are due to cloud cover, which was not represented in the model. It is not clear why the model flux is higher than the measurements. It is possible that the measurements underestimate the flux to some degree. For example, an error of $\pm 3\%(\times 700$ W $m^{-2} = 21$ W $m^{-2})$ in the measured flux could account for some of the differences shown.

The model may overestimate the solar flux due to insufficient aerosol absorption in the model. Increasing the black carbon content of the biomass-burning aerosol from 6 to 8% (by volume) reconciled the modelled flux with the measurements. This altered the single-scattering albedo from 0.87 to 0.83 (at 550 nm), which is just within the range expected from the FAAM and AERONET version 1 observations (see Table I). Increasing the AOD in the model by 0.1 or 15% also would have created agreement with the measurements but such an increase is not justified given that the model AOD was based on the Microtops sunphotometer, which should be accurate to within ± 0.02. Replacing 25% of the fine particles (radii $>$ 0.35 μm) with dust (rather than assuming all fine particles to be biomass-burning aerosol) led to an even greater overestimation of the downwelling solar flux in the model. This was caused by the higher single-scattering albedo of the aerosol mixture (0.90 at 550 nm). However, if the black carbon content of the biomass-burning aerosol was increased from 6 to 8% (restoring the overall black carbon content of the fine aerosol to 6%) then the single-scattering albedo and model results were virtually the same as before (the case assuming no fine dust).

The treatment of aerosols as spheres is another source of uncertainty which affects the calculation of aerosol optical properties used in the model. However, resulting errors in specific extinction coefficient will have been compensated for in this study since mass mixing ratios were constrained so that the column optical depth in the model matched that from the Microtops sunphotometer. Errors in single-scattering albedo and asymmetry parameter, resulting from the spherical assumption, were found to be negligible (Osborne *et al.*, 2008). Therefore, the discrepancies between the observed and measured flux in this study are more likely to be related to uncertainty in the single-scattering albedo than misrepresentation of particle shape, or uncertainty in AOD. In particular, we have not been able to constrain the spectral variation of single-scattering albedo in our model across all wavelengths, although comparison with AERONET over the 440–1020 nm range showed reasonable agreement. Other sources of model errors include uncertainties in the surface albedo (± 2 W m^{-2}), uncertainty in the water vapour profile (± 2 W m^{-2}) and the lack of stratospheric aerosol (not quantified). Discrepancies of a similar magnitude (~ 20 W m^{-2}) were also found for the 21 January 2006 case, examined by McFarlane *et al.* (2009), using aerosol optical properties derived solely from MFRSR measurements. As in the current study, they were able to attain agreement in fluxes by adjusting the aerosol optical properties in the radiative transfer model by 5–10%. These studies cannot be directly compared since they were conducted for different cases and used different surface flux measurements; however, they illustrate the general level of uncertainty in radiative flux closure studies under the conditions observed at Niamey.

8. Conclusions

A case-study from the DABEX campaign has been presented to investigate differences between *in situ* aircraft measurements, satellite retrievals and ground-based remote-sensing methods. The comparisons include data from the FAAM aircraft, the Banizoumbou AERONET site, a Microtops sunphotometer operated at Niamey, the ARM Mobile Facility at Niamey, the MISR satellite

DOI: 10.1002/qj

instrument and a new version (collection 5.1) of the MODIS Deep Blue algorithm. Airborne radiometer measurements and radiative transfer modelling are also used to assess the impact of aerosol on downwelling shortwave radiation. The case-study took place on 19 January 2006 over the region surrounding Niamey, Niger, which was the operating base of the FAAM aircraft during DABEX. Clear skies and high aerosol loadings make this an ideal case-study to test the performance of aerosol remote-sensing retrievals.

The aircraft measurements showed a shallow dust layer extending from the surface to 1 km and an elevated layer of biomass-burning aerosol between 1 and 3.5 km mixed with some dust. The single-scattering albedo at 550 nm varied from 0.98 in the dust layer to 0.82 in the upper parts of the biomass-burning aerosol layer. The AERONET and Microtops sunphotometers suggested an AOD of around 0.72–0.74 (at 550 nm) at the time of the aircraft measurements. The estimate of AOD from the aircraft (0.79) was in good agreement with the sunphotometers. *In situ* measurements suggest that biomass-burning aerosol and mineral dust were equally important contributors to the AOD at 550 nm. The MISR and MODIS Deep Blue satellite retrievals of AOD were within 10% of the sunphotometer measurements. This level of agreement was well within the expected uncertainty, given the difficulty of retrieving aerosol properties over brightly-reflective land surfaces, and aerosol variability convolved with sampling differences.

The derived optical properties from AERONET were in reasonable agreement with *in situ* measurements from the aircraft whereas the optical properties from MISR were somewhat at odds with the aircraft and AERONET. The AERONET retrieval suggested a column-average single-scattering albedo of 0.85 ± 0.03 (at 550 nm), which was close to the aircraft estimate of 0.87 ± 0.03. The MISR retrieval gave higher single-scattering albedos of 0.94 (at 550 nm) and also overestimated the AOD contribution from large particles ($r > 0.7$ μm) compared to AERONET. This is most likely due to the lack of sufficient mixtures of dust and absorbing spherical particles in the retrieval algorithm, thus choosing a dust mixture that had too little absorption and too few fine particles. This is consistent with previous MISR team analyses for other mixed dust and biomass-burning situations.

Measurements of downwelling solar radiation from the FAAM aircraft during a low-altitude run were reasonably in agreement with surface-based measurements from the AMF; differences averaged around 10 W m^{-2}. Radiative transfer model calculations were performed using aerosol optical properties and input profiles from the aircraft data. The model downwelling solar flux was about 20 W m^{-2} higher than the observations suggested, and this difference is most likely due to uncertainties in aerosol optical properties such as single-scattering albedo. This demonstrates the requirement for measurements of aerosol optical properties across a wider range of wavelengths to better constrain inputs, such as the refractive index, as a function of wavelength.

Acknowledgements

The FAAM aircraft is jointly funded by the Met Office and the Natural Environment Research Council. We thank Didier Tanré for his efforts in establishing and maintaining the Banizoumbou AERONET site, and Clare McConnell for processing the Microtops data. We thank Connor Flynn for his help with the MFRSR data, and Chuck Long and Yan Shi for processing the AMF radiometer data.

References

Alexandrov MD, Kiedron P, Michalsky JJ, Hodges G, Flynn CJ, Lacis AA. 2007. Optical depth measurements by shadow-band radiometers and their uncertainties. *Applied Optics* **46**: 8027–8038.

Anderson TL, Ogren JA. 1998. Determining aerosol radiative properties using the TSI 3563 integrating nephelometer. *Aerosol Sci. Technol.* **29**: 57–69.

Balkanski Y, Schulz M, Chaquin T, Guibert S. 2007. Reevaluation of mineral aerosol radiative forcings suggest a better agreement with satellite and AERONET data. *Atmos. Chem. Phys.* **7**: 81–95.

Bond TC, Anderson TL, Campbell D. 1999. Calibration and intercomparison of filter-based measurements of visible light absorption by aerosols. *Aerosol Sci. Technol.* **30**: 582–600.

Chen W-T, Kahn RA, Nelson D, Yau K, Seinfeld JH. 2008. Sensitivity of multiangle imaging to the optical and microphysical properties of biomass burning aerosols. *J. Geophys. Res.* **113**: D10203, DOI:10.1029/2007JD009414.

Chou C, Formenti P, Maille M, Ausset P, Helas G, Harrison M, Osborne S. 2008. Size distribution, shape, and composition of mineral dust aerosols collected during the African Monsoon Multidisciplinary Analysis Special Observation Period 0: Dust and Biomass-burning Experiment field campaign in Niger, January 2006. *J. Geophys. Res.* **113**: D00C10, DOI:10.1029/2008JD009897.

Christopher SA, Wang J. 2004. Intercomparison between multi-angle imaging spectroradiometer (MISR) and sunphotometer aerosol optical thickness in dust source regions over China: Implications for satellite aerosol retrievals and radiative forcing calculations. *Tellus* **56B**: 451–456.

Christopher SA, Gupta P, Haywood J, Greed G. 2008. Aerosol optical thicknesses over North Africa: 1. Development of a product for model validation using Ozone Monitoring Instrument, Multiangle Imaging Spectroradiometer, and Aerosol Robotic Network. *J. Geophys. Res.* **113**: D00C04, DOI:10.1029/2007JD009446.

Dubovik O, King MD. 2000. A flexible inversion algorithm for retrieval of aerosol optical properties from Sun and sky radiance measurements. *J. Geophys. Res.* **105**: 20673–20696.

Dubovik O, Sinyuk A, Lapyonok T, Holben BN, Mishchenko M, Yang P, Eck TF, Volten H, Muñoz O, Veihelmann B, van der Zande WJ, Leon J-F, Sorokin M, Slutsker I. 2006. Application of spheroid models to account for aerosol particle nonsphericity in remote sensing of desert dust. *J. Geophys. Res.* **111**: D11208, DOI:10.1029/2005JD006619.

Eck TF, Holben BN, Reid JS, Dubovik O, Smirnov A, O'Neil NT, Slutsker I, Kinne S. 1999. Wavelength dependence of the optical depth of biomass burning, urban, and desert dust aerosols. *J. Geophys. Res.* **104**: 31333–31350.

Eck TF, Holben BN, Ward DE, Mukelabai MM, Dubovik O, Smirnov A, Schafer JS, Hsu NC, Piketh SJ, Queface A, Le Roux J, Swap RJ, Slutsker I. 2003. Variability of biomass burning aerosol optical characteristics in southern Africa during the SAFARI 2000 dry season campaign and a comparison of single scattering albedo estimates from radiometric measurements. *J. Geophys. Res.* **108**: 8477, DOI:10.1029/2002JD002321.

Edwards JM, Slingo A. 1996. Studies with a flexible radiation code. I: Choosing a configuration for a large-scale model. *Q. J. R. Meteorol. Soc.* **122**: 689–719.

Formenti P, Rajot JL, Desboeufs K, Caquineau S, Chevallier S, Nava S, Gaudichet A, Journet E, Triquet S, Alfaro S, Chiari M, Haywood JM, Coe H, Highwood E. 2008. Regional variability of the composition of mineral dust from western Africa: Results from the AMMA SOP0/DABEX and DODO field campaigns. *J. Geophys. Res.* **113**: D00C13, DOI:10.1029/2008JD009903.

Harrison L, Michalsky J. 1994. Objective algorithms for the retrieval of optical depths from ground-based measurements. *Appl. Opt.* **33**: 5126–5132.

Haywood JM, Osborne SR, Francis PN, Keil A, Formenti P, Andreae MO, Kaye PH. 2003a. The mean physical and optical properties of regional haze dominated by biomass burning aerosol measured from the C-130 aircraft during SAFARI 2000. *J. Geophys. Res.* **108**: 8473, DOI:10.1029/2002JD002226.

Haywood JM, Francis PN, Osborne SR, Glew M, Loeb N, Highwood E, Tanré D, Myhre G, Formenti P, Hirst E. 2003b. Radiative properties and direct radiative effect of Saharan dust measured by the C-130 aircraft during SHADE: 1. Solar spectrum. *J. Geophys. Res.* **108**: 8577, DOI:10.1029/2002JD002687.

Haywood JM, Pelon J, Formenti P, Bharmal N, Brooks M, Capes G, Chazette P, Chou C, Christopher SA, Coe H, Cuesta J, Derimian Y, Desboeufs K, Greed G, Harrison M, Heese B, Highwood EJ, Johnson BT, Mallet M, Marticorena B, Marsham J, Milton S, Myhre G, Osborne SR, Parker DJ, Rajot J-L, Schulz M, Slingo A, Tanré D, Tulet P. 2008. Overview of the Dust and Biomass-burning Experiment and African Monsoon Multidisciplinary Analysis Special Observing Period-0. *J. Geophys. Res.* **113**: D00C17, DOI:10.1029/2008JD010077.

Heese B, Wiegner M. 2008. Vertical aerosol profiles from Raman polarization lidar observations during the dry season AMMA field campaign. *J. Geophys. Res.* **113**: D00C11, DOI:10.1029/2007JD009487.

Hsu NC, Tsay S-C, King MD, Herman JR. 2004. Aerosol properties over bright-reflecting source regions. *IEEE Trans. Geosci. Remote Sensing* **42**: 557–569.

Hsu NC, Tsay S-C, King MD, Herman JR. 2006. Deep Blue retrievals of Asian aerosol properties during ACE-Asia. *IEEE Trans. Geosci. Remote Sensing* **44**: 3180–3195.

Ichoku C, Levy R, Kaufman YJ, Remer LA, Li R-R, Martins VJ, Holben BN, Abuhassan N, Slutsker I, Eck TF, Pietras C. 2002. Analysis of the performance characteristics of the five-channel Microtops II Sun photometer for measuring aerosol optical thickness and precipitable water vapor. *J. Geophys. Res.* **107**: 4179, DOI:10.1029/2001JD001302.

IPCC (Intergovernmental Panel on Climatic Change). 2007. Changes in atmospheric constituents and in radiative forcing. In *Climate change 2007: The physical science basis. Contribution of Working Group I to the Fourth Assessment Report of the IPCC*, Solomon S, Qin D, Manning M, Chen Z, Marquis M, Avery KB, Tignor M, Miller HL (eds). Cambridge University Press: Cambridge, United Kingdom and New York.

Johnson BT, Osborne SR, Haywood JM, Harrison MAJ. 2008a. Aircraft measurements of biomass burning aerosol over West Africa during DABEX. *J. Geophys. Res.* **113**: D00C06, DOI:10.1029/2007JD009451.

Johnson BT, Heese B, McFarlane SA, Chazette P, Jones A, Bellouin N. 2008b. Vertical distribution and radiative effects of mineral dust and biomass burning aerosol over West Africa during DABEX. *J. Geophys. Res.* **113**: D00C12, DOI:10.1029/2008JD009848.

Kahn RA, Gaitley BJ, Martonchik JV, Diner DJ, Crean KA, Holben BN. 2005. Multiangle Imaging Spectroradiometer (MISR) global aerosol optical depth validation based on 2 years of coincident Aerosol Robotic Network (AERONET) observations. *J. Geophys. Res.* **110**: D10S04, DOI:10.1029/2004JD004706.

Kahn R, Petzold A, Wendisch M, Bierwirth E, Dinter T, Esselborn M, Fiebig M, Heese B, Knippertz P, Müller D, Schladitz A, Von Hoyningen-Huene W. 2009. Desert dust aerosol air mass mapping in the western Sahara using particle properties derived from space-based multi-angle imaging. *Tellus* **61B**: 239–251.

Kassianov EI, Flynn CJ, Ackerman TP, Barnard JC. 2007. Aerosol single-scattering albedo and asymmetry parameter from MFRSR observations during the ARM Aerosol IOP 2003. *Atmos. Chem. Phys.* **7**: 3341–3351.

Leahy LV, Anderson TL, Eck TF, Bergstrom RW. 2007. A synthesis of single scattering albedo of biomass burning aerosol over southern Africa during SAFARI 2000. *Geophys. Res. Lett.* **34**: L12814, DOI:10.1029/2007GL029697.

Liu Y, Daum PH. 2000. The effect of refractive index on size distributions and light scattering coefficients derived from optical particle counters. *J. Aerosol. Sci.* **31**: 945–957.

McClatchey RA, Fenn RW, Selby JEA, Volz FE, Garing JS. 1972. 'Optical properties of the atmosphere (Third Edition)'. Air Force Cambridge Research Laboratories, Report AFCRL-72-0497, Environmental Research Papers 411, Hanscom AFB, Massachusetts, USA.

McFarlane SA, Kassianov EI, Barnard J, Flynn C, Ackerman TP. 2009. Surface shortwave aerosol radiative forcing during the Atmospheric Radiation Measurement Mobile Facility deployment in Niamey, Niger. *J. Geophys. Res.* **114**: D00E06, DOI:10.1029/2008JD010491.

Martonchik JV, Diner DJ, Kahn RA, Gaitley BJ, Holben BN. 2004. Comparison of MISR and AERONET aerosol optical depths over desert sites. *Geophys. Res. Lett.* **31**: L16102, DOI:10.1029/2004GL019807.

Miller MA, Slingo A. 2007. The ARM Mobile Facility and its first international deployment: Measuring radiative flux divergence in West Africa. *Bull. Am. Meteorol. Soc.* **88**: 1229–1244.

Myhre G, Hoyle CR, Berglen TF, Johnson BT, Haywood JM. 2008. Modeling of the solar radiative impact of biomass burning aerosols during the Dust and Biomass-burning Experiment (DABEX). *J. Geophys. Res.* **113**: D00C16, DOI:10.1029/2008JD009857.

Osborne SR, Johnson BT, Haywood JM, Baran AJ, Harrison MAJ, McConnell CL. 2008. Physical and optical properties of mineral dust aerosol during the Dust and Biomass-burning Experiment. *J. Geophys. Res.* **113**: D00C03, DOI:10.1029/2007JD009551.

Remer LA, Kaufman YJ, Tanré D, Mattoo S, Chu DA, Martins JV, Li R-R, Ichoku C, Levy RC, Kleidman RG, Eck TF, Vermote E, Holben BN. 2005. The MODIS aerosol algorithm, products, and validation. *J. Atmos. Sci.* **62**: 947–973.

Slingo A, Bharmal NA, Robinson GJ, Settle JJ, Allan RP, White HE, Lamb PJ, Issa Lélé M, Turner DD, McFarlane SA, Kassianov E, Barnard J, Flynn C, Miller MA. 2008. Overview of observations from the RADAGAST experiment in Niamey, Niger: Meteorology and thermodynamic variables. *J. Geophys. Res.* **113**: D00E01, DOI:10.1029/2008JD009909.

WCP (World Climate Programme). 1986. *A preliminary cloudless standard atmosphere for radiation computation*. WCP-112, WMO/TD-No 24. World Meteorol. Organisation: Geneva.

Younkin K, Long CN. 2003. 'Improved correction of IR loss in diffuse shortwave measurements: An ARM value-added product'. ARM TR-009. http://www.arm.gov/publications/tech_reports/arm-tr-009.pdf.